Critical entropies for magnetic ordering in bosonic mixtures on a lattice

B. Capogrosso-Sansone,[1] Ş. G. Söyler,[2,3] N. V. Prokof'ev,[2,4] and B. V. Svistunov[2,4]
[1]*Institute for Theoretical Atomic, Molecular and Optical Physics, Harvard-Smithsonian Center of Astrophysics, Cambridge, Massachusetts 02138, USA*
[2]*Department of Physics, University of Massachusetts, Amherst, Massachusetts 01003, USA*
[3]*The Abdus Salam International Centre for Theoretical Physics, Strada Costiera 11, I-34151 Trieste, Italy*
[4]*Russian Research Center "Kurchatov Institute", 123182 Moscow, Russia*
(Received 10 December 2009; published 21 May 2010)

We perform a numeric study (Worm algorithm Monte Carlo simulations) of ultracold two-component bosons in two- and three-dimensional optical lattices. At strong enough interactions and low enough temperatures the system features magnetic ordering. We compute critical temperatures and entropies for the disappearance of the Ising antiferromagnetic and the *xy*-ferromagnetic order and find that the largest possible entropies per particle are $\sim 0.5 k_B$. We also estimate (optimistically) the experimental hold times required to reach equilibrium magnetic states to be on a scale of seconds. Low critical entropies and long hold times render the experimental observations of magnetic phases challenging and call for increased control over heating sources.

DOI: 10.1103/PhysRevA.81.053622 PACS number(s): 67.85.Hj, 67.85.Fg

I. INTRODUCTION

At the moment, one of the prominent focuses and major challenges of experiments with ultracold gases is the realization of configurations which can be used to study quantum magnetism [1,2]. Though interesting and fundamental on its own, better understanding of (frustrated) magnetic systems is further motivated by its relevance to high-T_c superconductivity and applications to quantum-information processing. Direct studies of condensed matter spin systems experimentally are limited by the lack of control over interactions, geometry, frustration, and contaminating effects of other degrees of freedom. A new approach consists of using ultracold atoms in optical lattices (OL) provided that the system is driven toward regimes where it is possible to map the corresponding (Bose-) Hubbard Hamiltonian to spin models.

Striking advances in experimental techniques (e.g., high controllability and tunability of Hamiltonian parameters) and, more recently, single site and single-particle imaging [3–6], brought forward the idea, originally proposed by Feynmann, of quantum simulation or emulation [7]. In the last decade, a considerable amount of theoretical and experimental research has been devoted to the objective of using ultracold lattice bosons and fermions to address many outstanding condensed matter problems via Hamiltonian modeling. Perhaps the biggest remaining experimental challenge consists of reaching low enough temperatures or entropies for the observation of ordered magnetic states. Theoretical insight on optimal conditions for such observations is greatly needed. While Mott-insulator (MI) phases of single-component bosonic systems have been observed experimentally [8–10], and finite-temperature effects have been extensively investigated recently [11–15], the multi-component case is still a work in progress [16,17] and, as of today, accurate results are lacking.

In the present work, we address the issue for the case of two-component bosonic systems. We obtain such important numbers as critical temperatures and, more importantly entropies, below which magnetic phases can be observed experimentally. With these numbers in hand, we provide rough estimates of hold times required for observing thermally equilibrated ordered magnetic states.

We consider a homogeneous system of two-component bosons in a cubic (square) lattice with repulsive inter species interaction and half-integer filling of each component. This system can be realized by loading OL with two different atomic species (see, e.g., experiments at LENS with rubidium and potassium mixtures [18,19]), or the same atomic species in two different internal energy states (see, e.g., recent experiments done at MIT [15] and experiments with state-dependent OL's done at Stony Brook University [20]). The inter- and intraspecies interaction strengths, $U_{ab} \equiv U$, U_{aa}, and U_{bb} can be tuned via Feshbach resonance or by changing the Wannier functions overlap (in the presence of state-dependent lattices). If the intraspecies interactions U_{aa} and U_{bb} are made much larger than any other energy scale, and the temperature is low enough, the system is accurately described by the two-component hard-core Bose-Hubbard Hamiltonian:

$$H = -t_a \sum_{\langle ij \rangle} a_i^\dagger a_j - t_b \sum_{\langle ij \rangle} b_i^\dagger b_j + U \sum_i n_i^{(a)} n_i^{(b)}. \quad (1)$$

Here $a_i^\dagger$ (a_i),$b_i^\dagger$ (b_i) are bosonic creation (annihilation) operators obeying the hard-core constraint $a_i^{\dagger 2} = b_i^{\dagger 2} = 0$, and t_a,t_b are hopping matrix elements for two species of bosons (A and B), respectively; the symbol $\langle \cdot \cdot \rangle$ imposes the nearest-neighbor constraint on the summation over site subscripts; $n_i^{(a)} = a_i^\dagger a_i$ and $n_i^{(b)} = b_i^\dagger b_i$.

Model (1) displays a very rich ground-state phase diagram [21–23] (see Fig. 1). For strong enough interactions, the system is incompressible in the particle-number sector (i.e., it is an MI). The remaining degree of freedom describing the boson type on a given site can be mapped onto the effective iso-spin variable [21,22,24] and gives rise to two possible MI states: a double checkerboard (2CB) solid phase, equivalent to the Ising antiferromagnet, and a super-counter-fluid (SCF), equivalent to a planar ferromagnet in the iso-spin terminology. For large enough hoppings the MI state undergoes a transition to a double-superfluid state (2SF). Finally, as it has been shown

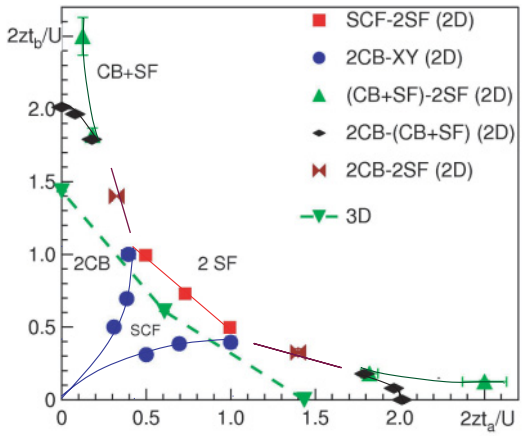

FIG. 1. (Color online) Phase diagram of model (1) on a square lattice and half-integer filling factor of each component (z is the coordination number). The 2CB-SCF first-order transition is represented by circles, the SCF-2SF second-order transition by squares, the 2CB-2SF first-order transition by stars, the 2CB-(CB + SF) second order transition by diamonds, and the (CB + SF)-2SF first-order transition by up triangles. Down triangles are benchmark points for the disappearance of magnetic order in the cubic lattice. Lines are to guide an eye.

recently [23], for strong asymmetry between the hopping amplitudes and relatively weak interspecies interaction a solid phase in the heavy component [25] is stabilized via a mechanism of inter-site effective interactions mediated by the (light) superfluid component. In what follows we will focus on the magnetic states, namely the Ising antiferromagnet and the (xy-)ferromagnet. We present the first precise results, based on path integral Monte Carlo (PIMC) simulations by the Worm algorithm [26], for transition lines to magnetic phases in two and three dimensions (2D and 3D) at zero and finite temperature, and discuss experimental parameters required for reaching them.

II. GROUND STATE

We begin with results for the ground state. In Fig. 1 we show the complete zero-temperature phase diagram of model (1) for the 2D system calculated in Ref. [23]. We also sketch (dashed line) the transition line for the disappearance of magnetic order for the 3D system by computing benchmark transition points (down triangles) for the strongly anisotropic and isotropic limits. These points correspond to the disappearance of the insulating Ising and the (xy-)ferromagnetic phases, respectively. While, as expected, the 3D case is better captured by the mean-field theory [22,23], the discrepancy between mean-field and Monte Carlo results is still sizable: ∼50%.

These results provide quantitative guidance for experimentally achieving the regime of quantum magnetism. In experiments with two different species this can be done by using Feshbach resonances [18] or by loading species-dependent lattices in order to reach the desired $t_{a,b}/U$ value; in the case of the same species but different internal states one can load state-dependent lattices and tune the interspecies interaction by changing the overlap of Wannier functions of the two components.

III. FINITE-TEMPERATURE RESULTS

Turning to the issue of reaching magnetic phases in realistic experimental setups—with an adiabatic protocol of turning on the optical lattice—we look for highest possible values of the critical entropy for the appearance of magnetically ordered states. The critical values of temperature come as a natural "by-product" of simulations. In what follows we use $t_b \geqslant t_a$ as the energy unit.

A. Critical temperatures

We start with the Ising antiferromagnet-to-normal transition. It belongs to the d-dimensional Ising universality class, the order parameter being the staggered magnetization along the z axis or, equivalently, in bosonic language, the structure factor (which is the square of the order parameter):

$$S_{\mathbf{K}}^{(a,b)} = \sum_{\mathbf{r},\mathbf{r}'} \exp[i\mathbf{K}\cdot(\mathbf{r}-\mathbf{r}')]\frac{\langle n_{\mathbf{r}}^{(a)} n_{\mathbf{r}'}^{(b)}\rangle}{N^{(a)}N^{(b)}}\,, \tag{2}$$

with $\mathbf{K}$ the reciprocal-lattice vector of the CB solid, that is, $\mathbf{K}=(\pi,\pi)$ in 2D and $\mathbf{K}=(\pi,\pi,\pi)$ in 3D, $n_{\mathbf{r}}^{(a,b)}$ the filling factor at the site $\mathbf{r}$, and $N^{(a,b)}$ the total number of particles A, B. In the vicinity of the transition point, the structure factor scales as

$$S_{\mathbf{K}}(\tau,L) = \xi^{-\frac{2\beta}{\nu}} f(\xi/L) = L^{-\frac{2\beta}{\nu}} g(\tau L^{\frac{1}{\nu}})\,, \tag{3}$$

where ξ is the correlation length, $\tau=(T-T_c)/t_b$ is the reduced temperature, L is the system size, assumed to be large enough to neglect higher-order corrections to the universal scaling, $f(x)$ and $g(x)$ are universal scaling functions, and β and ν are the critical exponent for the order parameter and correlation length, respectively. For the 2D case $2\beta/\nu=1/4$, and for the 3D case $2\beta/\nu=1.0366(8)$ [27]. At the critical point, the quantity $S_{\mathbf{K}}L^{2\beta/\nu}$ is size independent, provided L is appropriately large, and curves of different L's intersect. Figure 2 shows an example of the intersection for the case of a 2D system, with parameters $t_a/t_b=0.285$ and $U/t_b=5.7$,

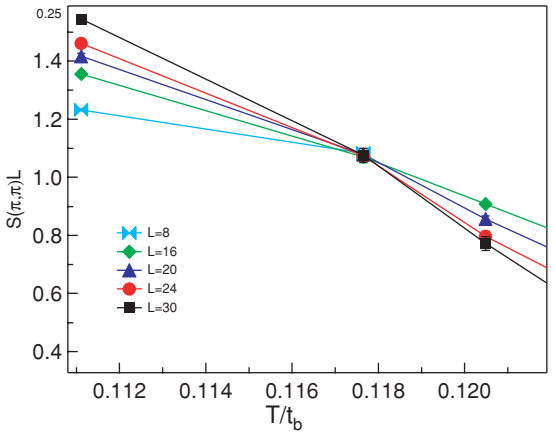

FIG. 2. (Color online) Finite-size scaling for the structure factor in the 2D system (see text) for $t_a/t_b=0.285$, $U/t_b=5.7$, and system sizes $L=8,16,20,24,30$. The critical temperature can be read from the intersection of curves corresponding to different L's. Lines are a guide to the eye.

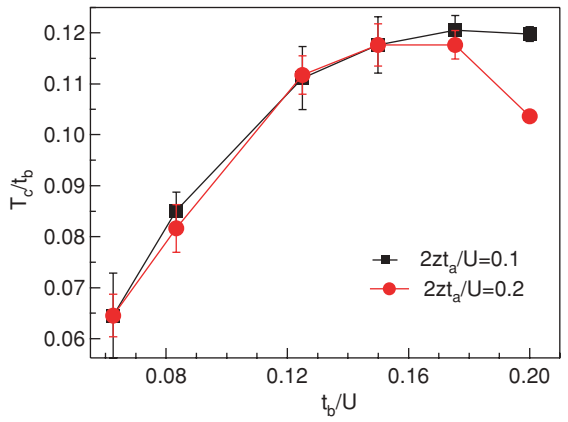

FIG. 3. (Color online) Critical temperature for the Ising state versus t_a/U in the 2D system at fixed $2zt_b/U = 0.1$ and 0.2, squares and circles, respectively. Lines are a guide to the eye.

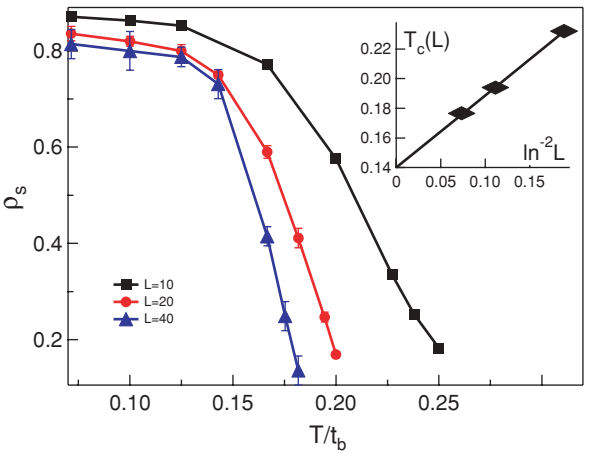

FIG. 4. (Color online) (Main plot) Superfluid stiffness of the particle-hole composite object in the SCF (*xy*-ferromagnetic) state with $t_a = t_b$ and $U/t_b = 11$ for system sizes $L = 10,20,40$ triangles, circles, and squares, respectively. (Inset) Scaling of the finite-size "critical temperature" (see text).

and system sizes $L = 8,16,20,24,30$. The critical temperature is $T_c/t_b = 0.1175(10)$.

Our results for critical temperatures in 2D are summarized in Fig. 3. We have performed simulations at fixed $2zt_a/U = 0.1,0.2$ and varying t_b/U. Our data show that the region with higher transition temperatures corresponds to relatively weak interactions, but away from the transition to the (CB + SF) ground state. For strong interactions, the relevant energies (i.e., coupling of spin degrees of freedom in the mapping to the quantum spin Hamiltonian) scale as $\propto U^{-1}$, and therefore require smaller temperatures in order to stabilize magnetically ordered phases. On the other hand, for weak enough interactions, the magnetic order will eventually disappear in favor of the (CB + SF) phase. As we approach this transition the magnetic order becomes weaker, therefore lower temperatures are required to observe it though the effect is rather moderate. The largest transition temperatures lie somewhere in between these two limits, and with precise numerical simulations it is possible to accurately pinpoint the parameter region which is best suited for current experiments. The largest critical temperatures we have observed are $T_c/t_b \sim 0.12$.

In the 3D case, we have calculated T_c in the region where we expect it to be large, $U/t_b = 11$, $t_a/t_b = 0.1$. We have found $T_c/t_b = 0.175(15)$. The 3D simulations are far more demanding computationally than in 2D, and the calculation of the full zero- and finite-temperature phase diagram in 3D is beyond the scope of this work.

We now turn to the melting of the *xy*-ferromagnetic state. In bosonic language, it corresponds to the SCF-to-normal transition where SCF is characterized as the superfluid state with the composite order parameter describing the condensate of pairs consisting of particles of one component and holes of the other one, with zero net particle flux. The transition is of the d-dimensional U(1) universality class, meaning that in 2D it is of the Kosterlitz-Thouless (KT) type. In Fig. 4 we show an example of how transition points for the 2D system are calculated. In order to locate the critical temperature we employ finite-size arguments following from KT renormalization-group flow for the superfluid stiffness ρ_s, the latter being measured from statistics of fluctuations of winding numbers [28]:

$$\rho_s = \frac{\langle \mathbf{W}^2 \rangle}{\beta L^{d-2}}, \tag{4}$$

where $\mathbf{W}$ is the vector of world-line winding numbers in the SCF sector. For our purposes, it is sufficient to define ρ_s up to a global prefactor; that is why our Eq. (4) contains no other factors.

In terms of world-line windings, the universal Nelson-Kosterlitz jump translates into the abrupt change of $\langle \mathbf{W}^2 \rangle$ at the critical point from $4/\pi$ in the SCF phase to zero in the normal phase. In a finite system, the universal jump is smoothed out and winding numbers go to zero continuously (see the main plot in Fig. 4). If one defines the finite-size critical point $T_c(L)$ by the condition $\langle \mathbf{W}^2[T_c(L)] \rangle = 4/\pi$, then the flow of $T_c(L)$ to the thermodynamic limit answer $T_c = T_c(\infty)$ is given by $T_c(L) - T_c \propto 1/(\ln L)^2$; see the inset in Fig. 4.

We have found the following critical temperatures: $T_c/t_b = 0.141(5)$ for $U/t_b = 11$, $t_a/t_b = 1$; $T_c/t_b = 0.104(5)$ for $U/t_b = 13$, $t_a/t_b = 1$; $T_c/t_b = 0.101(5)$ for $U/t_b = 11$, $t_a/t_b = 0.8$; $T_c/t_b = 0.14(1)$ for $U/t_b = 9.4$, $t_a/t_b = 0.6$. Critical temperatures seem to decrease as we go toward the Heisenberg point and the effective iso-spin couplings decrease (see argument above). Unlike the Ising-normal transition, the highest transition temperature we have found lies close to the SCF-2SF $T = 0$ transition line. In fact, across this transition line the superfluid stiffness of the particle-hole composites and the transition temperature to the normal state remain finite. As discussed in Ref. [29], at finite temperature the SCF-2SF boundary moves in the direction of the 2SF ground state thus implying the following sequence of events: as temperature is increased in the vicinity of the quantum critical point the 2SF state first undergoes a transition to the SCF state which then turns normal at a much higher temperature.

In the 3D case, the transition point can be obtained from the finite-size scaling of ρ_s. Similarly to Eq. (3), one has

$$\rho_s(\tau, L) = \xi^{-1} f(\xi/L) = L^{-1} g(\tau L^{\frac{1}{\nu}}). \tag{5}$$

The critical temperature is extracted from the intersection of $\rho_s(\tau,L)L$ curves. We have done simulations for the system parameters $U/t_b = 21, t_a/t_b = 1$ and found $T_c/t_b = 0.208(7)$.

B. Entropy curves

Entropy curves $S(T)$ are calculated starting from the energy data. We first use spline interpolation of data points to obtain a smooth curve $E(T)$. We then calculate entropy by using two different numerical procedures: (i) We obtain the specific heat c_V by differentiating the spline and then calculate the entropy by numerical integration of c_V/T. (ii) We avoid numerical derivatives by using

$$S(T) = \frac{E(T) - E(0)}{T} + \int_0^T \frac{E(T) - E(0)}{T^2}\, dT, \qquad (6)$$

and numerical integration. The agreement of the two methods is very good (within 0.5%). Uncertainties in entropies come therefore from the ones in critical temperatures and finite-size effects. Examples of entropy curves in the Ising antiferromagnetic state are shown in Fig. 5, for $U/t_b = 5.7$, $t_a/t_b = 0.1425$ in 2D, and $U/t_b = 11$, $t_a/t_b = 0.1$ in 3D. We find critical entropies per particle $S_c(k_B)/N \sim 0.25 \pm 5\%$ and $0.5 \pm 20\%$ in 2D and 3D, respectively. These entropies are relatively large and definitely within the realm of what can be achieved with bosonic BECs. In Fig. 6 we show entropy curves for the xy-ferromagnetic state. The critical entropy in 2D for $U/t_b = 11$, $t_a/t_b = 1$ is $S_c(k_B)/N \sim 0.033 \pm 5\%$, about an order of magnitude smaller than for the 3D value $S_c(k_B)/N \sim 0.35 \pm 10\%$ obtained for $U/t_b = 21$, $t_a/t_b = 1$. This is explained by the specifics of the KT transition when the SF density jumps to zero discontinuously at the critical point (i.e., when the system thermodynamics is still dominated by the dilute phonon gas). Correspondingly, at the transition temperature the thermal energies and entropies are low. Our thermodynamic data confirm that this is precisely what is happening for the 2D system: energy scales with temperature as $\propto T^3$ (which implies that entropy is $\propto T^2$) all the way up to temperatures $T < T_c$.

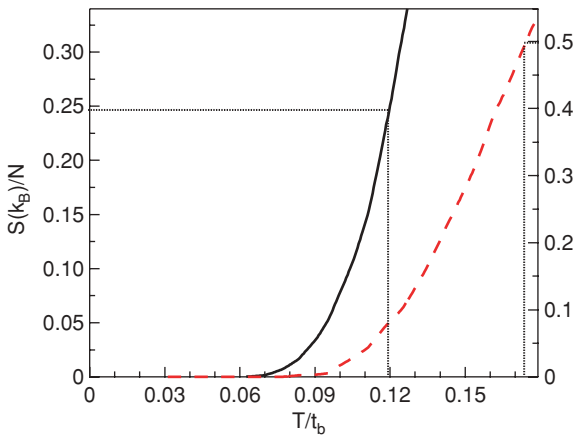

FIG. 5. (Color online) Entropy curves for the Ising antiferromagnet in 2D for $U/t_b = 5.7$, $t_a/t_b = 0.142$ and 3D for $U/t_b = 11$, $t_a/t_b = 0.1$, solid and dashed lines, respectively. Dotted lines are a guide to the reading of critical entropies.

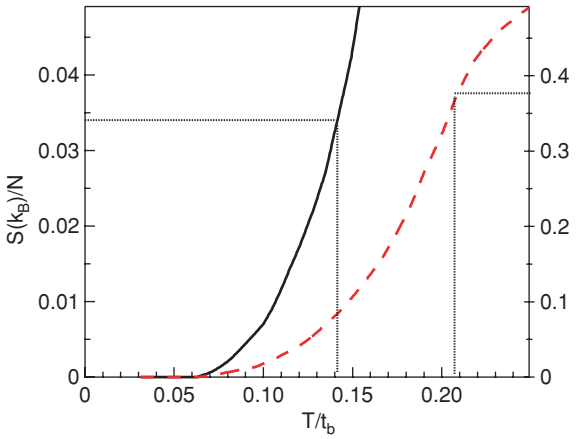

FIG. 6. (Color online) Entropy curves for the xy ferromagnet in 2D for $U/t_b = 11$, $t_a/t_b = 1$ and 3D for $U/t_b = 21$, $t_a/t_b = 1$, solid and dashed lines, respectively. Dotted lines are a guide to the reading of critical entropies.

IV. MINIMAL EXPERIMENTAL HOLD TIMES

Finally, we estimate minimal hold times required to observe ordered magnetic phases under typical experimental conditions.

For a cubic lattice and using a harmonic approximation around the minima of the optical lattice potential [30], the tunneling matrix elements and on-site interaction energies are given by

$$t_{a,b} \approx \frac{4}{\sqrt{\pi}} \left(E_R^{(a,b)} V_{a,b}^3\right)^{\frac{1}{4}} \exp\left(-2\sqrt{V_{a,b}/E_R^{(a,b)}}\right), \qquad (7)$$

$$U \approx \frac{4\sqrt{\hbar}}{\sqrt{\pi}}\, a_s^{(ab)}\, \overline{m\omega}^{3/2} \frac{1}{2\nu_{ab}}, \qquad (8)$$

$$U_{a,b} \approx \frac{\sqrt{2\hbar}}{\pi}\, a_s^{(aa,bb)} (m_{a,b}\omega_{a,b})^{3/2} \frac{1}{m_{ab}}, \qquad (9)$$

where

$$\overline{m\omega} = \frac{m_a\omega_a m_b\omega_b}{m_a\omega_a + m_b\omega_b}, \qquad (10)$$

and

$$\omega_{a,b} = \sqrt{4E_R^{(a,b)} V_0^{a,b}}/\hbar \qquad (11)$$

is the harmonic oscillator frequency,

$$E_R^{(a,b)} = \frac{\hbar^2 k^2}{2m_{a,b}} \qquad (12)$$

is the atomic recoil energy, $m_{a,b}$ and ν_{ab} are the bare and reduced masses, respectively, and $a_s^{(aa,bb)}$ and $a_s^{(ab)}$ are the intra- and interspecies scattering lengths. The hard-core limit can be achieved if, for example, $a_s^{(aa,bb)} \gg a_s^{(ab)}$, or by manipulation of the overlapping of Wannier functions, whereas resonances are not available. For ^{87}Rb-^{41}K mixtures [18] and away from resonances one has $a_{\text{Rb-K}} = 163a_0$, $a_{\text{Rb}} = 99a_0$, and $a_{\text{K}} = 65a_0$ (a_0 is the Bohr radius). One can then use Feshbach resonances to tune scattering lengths to the hard-core limit. This can be done by either using the resonance for interspecies collisions (it is possible to tune the scattering length through the zero point crossing [18,19], thus realizing

the hard-core constraint) or by exploiting resonances for collisions within the same species. As we will see below, the latter case corresponds to shorter experiment hold times.

To estimate the hold time $t_{\rm expt}$ required for the observation of the magnetic phases we look at the lowest dynamic energy scale in the system which is t_a in our case. Clearly, unless a condition $t_{\rm expt} \gg h/t_a$ is satisfied, one may not even discuss thermally equilibrated normal states, not to mention low-temperature ordered ones. If T_c is smaller than t_a, we consider $t_{\rm expt} \gg h/T_c$ as the minimal requirement. As we have seen, the optimal experimental parameters for both Ising and xy phases result in $\min(t_a, T_c) \sim 0.1 t_b$, and in what follows we will use this energy scale for the estimate of the hold time.

Let us consider laser beams with $\lambda = 1064$ nm and discuss the mixtures of Rb atoms in states $|1,-1\rangle$ and $|2,-2\rangle$ [15,20], for which $a_s^{(ab)} = 98.09 a_0$. For the melting of the Ising state we require $U/t_b \sim 11$ and $t_a/t_b \sim 0.1$ which translates into the optical lattice depths $V_a/E_R^{(a)} \sim 19.5$ and $V_b/E_R^{(b)} \sim 9$, and the final result $t_{\rm expt} \gg 0.2$ s. For the melting of the (xy-)ferromagnet we require $U/t_b \sim 21$, $t_a \sim t_b$, or, in terms of the lattice depths, $V_a/E_R^{(a)} = V_b/E_R^{(b)} \sim 12$, which implies that $t_{\rm expt} \gg 0.035$ s. For the case of ^{87}Rb-^{41}K mixtures, the best-case scenario corresponds to $a_{\text{Rb-K}} = 163 a_0$ and $a_{\rm Rb}, a_{\rm K} \gg a_{\text{Rb-K}}$ achieved via Feshbach resonances for intraspecies collisions. We consider the b species to be ^{87}Rb. A similar analysis of the Ising antiferromagnetic case leads to $V_a/E_R^{(a)} \sim 19.5$, $V_b/E_R^{(b)} \sim 6$, and $t_{\rm expt} \gg 0.08$ s. For the xy-ferromagnetic case we have $V_a/E_R^{(a)} \sim 11.5$ and $V_b/E_R^{(b)} \sim 8.6$ and $t_{\rm expt} \gg 0.015$ s. If, instead, one tunes the interspecies scattering length to, for example, $a_{\text{Rb-K}} \sim 35 a_0$, this implies $V_a/E_R^{(a)} \sim 26.2$, $V_b/E_R^{(b)} \sim 10.6$, $t_{\rm expt} \gg 0.25$ s for the Ising antiferromagnet, and $V_a/E_R^{(a)} \sim 17.3$, $V_b/E_R^{(b)} \sim 13.6$, $t_{\rm expt} \gg 0.05$ s for the (xy-)ferromagnet. Smaller interspecies scattering lengths would require even longer hold times, hence it results experimentally more feasible to enforce the hard-core limit by tuning the intraspecies scattering lengths.

From these estimates we conclude that observing ordered magnetic phases will be experimentally challenging since the required time scales might have to exceed seconds (with some advantage for dealing with the ^{87}Rb-^{41}K mixture). Increasing the sample stability and suppressing various heating mechanisms (three-body losses, background vacuum, spontaneous scattering of lattice photons, and technical noises such as beam alignment, intensity fluctuations, mechanical vibrations) has to be achieved. To appreciate the problem, we mention the heating rate (entropy per particle) of $\sim 1 k_B$/s observed recently in a typical experiment in the optical lattice [11]. It is also important to realize that the hard-core limit studied in the present work corresponds to the best-case (i.e., largest critical entropies) scenario. The Mott-insulator region, where the magnetic order is realized, shrinks as one moves away form the hard-core limit [22], implying lower critical temperatures or entropies.

V. CONCLUSION

We have addressed numerically (by worm algorithm Monte Carlo simulations) the problem of magnetic ordering in the two-component Bose-Hubbard model in the intraspecies hard-core limit, for 2D and 3D cases, at finite temperature. The emphasis of the study is on revealing the optimal parameters for (and analyzing the feasibility of) experimentally achieving the transitions to Ising antiferromagnetic (or checkerboard solid) and xy-ferromagnetic (or super-counter-fluid) phases. We have identified the optimal experimental conditions, corresponding to maximal critical entropy per particle. On the basis of our data, we have estimated minimal experimental hold times required to reach equilibrium magnetic states. These times have to be on a scale of seconds which renders the experimental observations of magnetic phases challenging and calls for increased control over heating sources.

Our results—optimal Hamiltonian parameters with corresponding values of critical entropies, temperatures, and minimal hold times—can be directly used for guiding and benchmarking the ongoing experiment on creating optical lattice emulators.

ACKNOWLEDGMENTS

We thank D. Schneble, D. Pertot, B. Gadway, F. Minardi, M. Inguscio, J. Catani, G. Lamporesi, G. Barontini, G. Thalahammer, W. Ketterle, D. Weld, and H. Miyake for fruitful discussions. This work was supported by the Institute for Theoretical Atomic and Molecular Physics, the Defense Advanced Research Projects Agency Optical Lattice Emulator program, and the National Science Foundation (Grant No. PHY-0653183).

[1] S. Sachdev, Nat. Phys. **4**, 173 (2008).
[2] M. Lewenstein, A. Sanpera, V. Ahufinger, B. Damski, A. Sen(De), and U. Sen, Adv. Phys. **56**, 243 (2007).
[3] W. S. Bakr, J. I. Gillen, A. Peng, S. Foelling, and M. Greiner, Nature **462**, 74 (2009).
[4] A. Klinger, S. Degenkolb, N. Gemelke, K. Brickman Soderberg, and C. Chin, Rev. Sci. Instrum. **81**, 013109 (2010).
[5] K. D. Nelson, X. Li, and D. S. Weiss, Nat. Phys. **3**, 556 (2007).
[6] P. Würtz, T. Langen, T. Gericke, A. Koglbauer, and H. Ott, Phys. Rev. Lett. **103**, 080404 (2009).
[7] R. P. Feynmann, Int. J. Theor. Phys. **21**, 467 (1982).
[8] M. Greiner, M. O. Mandel, T. Esslinger, T. Hänsch, and I. Bloch, Nature **415**, 39 (2002).
[9] I. B. Spielman, W. D. Phillips, and J. V. Porto, Phys. Rev. Lett. **98**, 080404 (2007).
[10] I. Bloch, J. Dalibard, and W. Zwerger, Rev. Mod. Phys. **80**, 885 (2008).
[11] S. Trotzky, L. Pollet, F. Gerbier, U. Schnorrberger, I. Bloch, N. V. Prokof'ev, B. Svistunov, and M. Troyer, e-print arXiv:0905.4882 [cond-mat].
[12] L. Pollet, C. Kollath, K. Van Houcke, and M. Troyer, New J. Phys. **10**, 065001 (2008).
[13] Q. Zhou and T.-L. Ho, e-print arXiv:0908.3015 [cond-mat].
[14] B. Capogrosso-Sansone, N. V. Prokof'ev, and B. V. Svistunov, Phys. Rev. B **75**, 134302 (2002).

[15] D. M. Weld, P. Medley, H. Miyake, D. Hucul, D. E. Pritchard, and W. Ketterle, Phys. Rev. Lett. **103**, 245301 (2009).
[16] S. Powell, Phys. Rev. A **79**, 053614 (2009).
[17] A. Hubener, M. Snoek, and W. Hofstetter, Phys. Rev. B **80**, 245109 (2009).
[18] J. Catani, L. De Sarlo, G. Barontini, F. Minardi, and M. Inguscio, Phys. Rev. A **77**, 011603 (2007).
[19] G. Thalhammer, G. Barontini, L. De Sarlo, J. Cartani, F. Minardi, and M. Inguscio, Phys. Rev. Lett. **100**, 210402 (2008).
[20] B. Gadway, D. Pertot, R. Reimann, and D. Schneble, e-print arXiv:1002.4015 [cond-mat.quant-gas].
[21] A. B. Kuklov and B. V. Svistunov, Phys. Rev. Lett. **90**, 100401 (2003).
[22] E. Altman, W. Hofstetter, E. Demler, and M. D. Lukin, New J. Phys. **5**, 113 (2003).
[23] S. G. Söyler, B. Capogrosso-Sansone, N. V. Prokof'ev, and B. V. Svistunov, New J. Phys. **11**, 073036 (2009).
[24] M. Boninsegni, Phys. Rev. Lett. **87**, 087201 (2001).
[25] After this phase was revealed in Ref. [23], Hubener *et al.* [17] attempted to interpret it as a supersolid. We find this interpretation deeply misleading. In a single-component system, supersolid is defined as a state with spontaneously broken translational symmetry that is able to support the superflow of its particles. Clearly, for the definition to remain nontrivial in the multicomponent case, the superflow requirement should apply to *each* component of the system. Otherwise, the superconductors will immediately fall under the category of supersolids. Furthermore, one would be bound to use the term supersolid in the context of heterogeneous systems involving a solid and a superfluid subsystems, like superfluid helium in porous media, superfluid helium films on solid substrates, and even Wigner crystals of electrons on the surface of superfluid helium.
[26] N. V. Prokof'ev, B. V. Svistunov, and I. S. Tupiysyn, Phys. Lett. A **238**, 253 (1998); Sov. Phys. JETP **87**, 310 (1998).
[27] M. Hasenbusch, K. Pinn, and S. Vinti, Phys. Rev. B **59**, 11471 (1999).
[28] D. M. Ceperley and E. L. Pollock, Phys. Rev. B **36**, 8343 (1987).
[29] A. Kuklov, N. V. Prokof'ev, and B. V. Svistunov, Phys. Rev. Lett. **92**, 030403 (2004).
[30] D. Jacksch, C. Bruder, J. I. Cirac, C. W. Gardiner, and P. Zoller, Phys. Rev. Lett. **81**, 3108 (1998).